

# Temperature and pH mediate stoichiometric constraints of organically derived soil nutrients

Ligia F. T. de Souza  | Sharon A. Billings 

Department of Ecology and Evolutionary Biology, Kansas Biological Survey & Center for Ecological Research, University of Kansas, Lawrence, Kansas, USA

## Correspondence

Ligia F. T. de Souza, Department of Ecology and Evolutionary Biology, Kansas Biological Survey & Center for Ecological Research, University of Kansas, Lawrence, KS, USA.  
Email: [ligiaftsouza@ku.edu](mailto:ligiaftsouza@ku.edu)

## Funding information

National Institute of Food and Agriculture, Grant/Award Number: 2021-67019-34338; National Science Foundation, Grant/Award Number: EAR-2026874 and OIA-1656006; Kansas Board of Regents; University of Kansas Field Station

## Abstract

It remains unclear how warming will affect resource flows during soil organic matter (SOM) decomposition, in part due to uncertainty in how exoenzymes produced by microbes and roots will function. Rising temperatures can enhance the activity of most exoenzymes, but soil pH can impose limitations on their catalytic efficiency. The effects of temperature and pH on enzyme activity are often examined in environmental samples, but purified enzyme kinetics reveal fundamental attributes of enzymes' intrinsic temperature responses and how relative release of decay-liberated resources (their flow ratios) can change with environmental conditions. In this paper, we illuminate the principle that fundamental, biochemical limitations on SOM release of C, N, and P during decay, and differential exoenzymes' responses to the environment, can exert biosphere-scale significance on the stoichiometry of bioavailable soil resources. To that end, we combined previously published intrinsic temperature sensitivities of two hydrolytic enzymes that release C and N during decay with a novel data set characterizing the kinetics of a P-releasing enzyme (acid phosphatase) across an ecologically relevant pH gradient. We use these data to estimate potential change in the flow ratios derived from these three enzymes' activities (C:N, C:P, and N:P) at the global scale by the end of the century, based on temperature projections and soil pH distribution. Our results highlight how the temperature sensitivity of these hydrolytic enzymes and the influence of pH on that sensitivity can govern the relative availability of bioavailable resources derived from these enzymes. The work illuminates the utility of weaving well-defined kinetic constraints of microbes' exoenzymes into models that incorporate changing SOM inputs and composition, nutrient availability, and microbial functioning into their efforts to project terrestrial ecosystem functioning in a changing climate.

## KEY WORDS

acid phosphatase, flow ratios, global change, *N*-acetyl-glucosaminidase, nutrient availability, soil enzyme activity, soil pH, warming,  $\beta$ -glucosidase

This is an open access article under the terms of the Creative Commons Attribution-NonCommercial License, which permits use, distribution and reproduction in any medium, provided the original work is properly cited and is not used for commercial purposes.

© 2021 The Authors. *Global Change Biology* published by John Wiley & Sons Ltd.

## 1 | INTRODUCTION

Understanding how varying temperature affects nutrient provision to biota is necessary for predicting ecosystem services under climate change (Conant et al., 2011; Sardans et al., 2012). Because diverse soil processes that influence ecosystem feedbacks to climate such as organic matter decomposition (Conant et al., 2011; von Lützow & Kögel-Knabner, 2009) and soil microbial respiration (Bradford et al., 2008; Davidson & Janssens, 2006) can exhibit different temperature sensitivities in diverse environmental conditions, projecting soil resource flows with climate change is challenging. Soil exoenzyme activities are often used as a proxy of potential decay rates to investigate the relative rates at which resources may become available during decay, as they mediate the degradation and subsequent availability of resources comprising soil organic matter (SOM; Sinsabaugh, 2010; Wallenstein & Weitraub, 2008).

One challenge in predicting the responses of exoenzymes to changing temperatures is that their temperature sensitivity is affected by soil pH, which can change enzyme conformation and adsorption to soil colloids, in addition to modifying the solubility of substrates (Quiquampoix, 2000; Zimmerman & Ahn, 2010). As a result, different enzymes can exhibit unique responses to temperature at different pH (Min et al., 2014), which can create shifting stoichiometries of resources liberated upon decay (Lehmeier et al., 2013; Min et al., 2014). This concept is important for projections of decay-promoted resource availability, given lateral and vertical soil pH variation (Hengl et al., 2017), and because soil pH can change not only with climate (Slessarev et al., 2016) but also with agricultural intensification (Malik et al., 2018) and restoration practices (Berthrong et al., 2009) on timescales of years to decades. Moreover, changes in the active sites of enzymes with soil pH affect substrate binding and can constrain the temperature sensitivity of their interactions, a feature that may even lead to negative effects of warming on enzyme activities (Bárta et al., 2014; Steinweg, Jagadamma et al., 2013). However, few studies address how varying soil pH can impact soil exoenzyme activity (Min et al., 2014; Puissant et al., 2019), in spite of our knowledge that the pH optima of hydrolytic exoenzymes vary significantly (German et al., 2011; Min et al., 2014) and can be a limiting factor for decomposition (Sinsabaugh, 2010).

The ratio of organically bound resources liberated by enzyme activity during decay—the “flow ratio” (Billings & Ballantyne, 2013)—can serve as a fundamental stoichiometric constraint for ecosystem processes (Bárta et al., 2014; Billings & Ballantyne, 2013; Lehmeier et al., 2013). How a flow ratio may change with temperature and pH can be assessed by estimating the change in exoenzyme responses to these variables (Lehmeier et al., 2013; Min et al., 2014). Purified, isolated enzyme responses are especially valuable because these kinetics are free from the confounding effects of site-specific soil and microbial properties. As such, they can represent fundamental enzyme kinetics in a diversity of soil types and thus offer a means of constraining microbial processes in Earth system models (ESMs) attempting to project soil biogeochemical dynamics in a rapidly changing climate (Wieder et al., 2015). Moreover, flow ratios derived from

purified enzymes can provide a mechanistic glimpse into how the phenomenon of changing stoichiometries of bioavailable resources can occur as environmental conditions change. Developing such a module can contribute to ongoing efforts to improve projections of soil C through ESMs (Luo et al., 2016; Wieder et al., 2018) by addressing how the interactions between C, N, and P may constrain future terrestrial productivity (Reed et al., 2015; Sokolov et al., 2008; Sun et al., 2017; Thornton et al., 2007; Wang et al., 2010; Zaehle et al., 2010).

Here, we aimed to demonstrate the potential for key biochemical limitations during SOM decay to influence the rate at which resources become available at large spatial scales. Using global maps of soil pH at multiple depths (Hengl et al., 2017) and temperatures projected through 2100 from the Coupled Model Intercomparison Project Phase 6 (CMIP6; Eyring et al., 2016), we projected relative changes in C, N, and P released by three soil exoenzymes during substrate decay as pH and temperature varies. We obtained kinetic data for C- and N-releasing enzymes from the literature (Min et al., 2014). Using the kinetics defined by published and newly generated data, we calculated C:N, C:P, and N:P flow ratios across a range of pH, and transformed these flow ratios into spatially explicit, initial estimates of relative changes with temperature of organically derived C, N, and P resources released by these three hydrolytic enzymes at three soil depths at the global scale. These estimates are independent of the influence of temperature and pH on microbial community composition, plant nutrient demand, and edaphic properties other than pH and thus represent the biochemical potential of these exoenzymes to generate bioavailable C, N, and P as only temperature and pH vary. Diverse chemical and physical edaphic attributes, microbial responses to environmental conditions, and substrate availabilities over time conspire to limit the accuracy of projections of the rates at which C, N, and P become bioavailable in any soil. However, this work offers proof-of-concept that the relative temperature sensitivities of diverse decay reactions as environmental conditions vary can sculpt stoichiometric constraints at a biosphere scale and represents a first step towards constraining those phenomena in ESMs.

## 2 | MATERIALS AND METHODS

### 2.1 | Global maps of projected change in the C:N, C:P, and N:P flow ratios

To create spatially explicit estimates of flow ratios of C:N, C:P, and N:P, we first projected activities of C- and N-releasing enzymes reported by Min et al. (2014;  $\beta$ -glucosidase, BGase, and N-acetylglucosaminidase, NAGase, respectively) and activities of acid phosphatase (APase) characterized *de novo* for this study (Appendix A in Supporting Information) for different past and future climate scenarios by parameterizing the Arrhenius equation at multiple pH:

$$K = A \times e^{(-\frac{E_a}{RT})} \quad (1)$$

where  $K$  describes the reaction rates,  $A$  is a pre-exponential factor,  $E_a$  is the activation energy,  $R$  is the universal gas constant, and  $T$  is the temperature in degrees Kelvin (Arrhenius, 1889; Knorr et al., 2005). The temperature sensitivity (i.e., the activation energy) of each enzyme is determined by fitting a linear regression using the Arrhenius-transformed specific activity of the enzymes ( $\ln(\text{specific activity}) \times R$ ; see Equation 1) as the response, pH as a categorical predictor, and temperature (as  $1/T$ ) as a covariate. For each pH, the slopes correspond to an estimate of  $E_a$  and the intercepts are an estimate of the pre-exponential factor  $A$  (Min et al., 2014).

We downloaded trends of mean annual temperature (MAT) with spatial resolution of 2.5 min from the WorldClim database (version 2.1 released in January 2020, <https://www.worldclim.org/>; Fick & Hijmans, 2017). The historical MAT data are represented as an annual trend from 1970 to 2000 (Fick & Hijmans, 2017), and the future climate data are downscaled projections of MATs from 2081 to 2100 by the CMIP6 (Eyring et al., 2016) for eight different global climate models and two emission scenarios driven by different socioeconomic assumptions (Table S1), or "Shared Socioeconomic Pathways" (SSPs; SSP2-4.5, SSP5-8.5; Gidden et al., 2019).

We obtained the global distribution of soil pH at 250 m from the SoilGrids database (<https://soilgrids.org/>, February 2017; Hengl et al., 2017) for three depths: 0, 30, and 100 cm. We focused on regions where soil pH was between 4.5 and 7.5, the common pH interval across which purified enzyme kinetics are reported here are in Min et al. (2014).

Using ArcMap 10.7.1 (ESRI, 2019), we transformed all temperature data sets from degree Celsius to kelvin using the *Raster Calculator* tool, and we matched the soil pH data sets to their spatial resolution of 2.5 min using the "Cell Size Projection Method" setting as "Preserve Resolution" in the *Raster Analysis* geoprocessing environment. Therefore, the data sets used to calculate the estimated enzyme activity globally have the same spatial resolution of 2.5 min.

We created spline functions based on the specific activity data set for the three enzymes of interest. This function allowed us to predict  $E_a$  and  $A$  for any pH value between 4.5 and 7.5, and thus for us to create spatially explicit estimates of  $E_a$  and  $A$  for each depth. We combined these estimates of  $E_a$  and  $A$  with the CMIP6-derived temperature data sets and the gas constant  $R$  to project enzyme activity (i.e., reaction rates) globally using the Arrhenius equation (Equation 1) at 0, 30, and 100 cm deep. Both the spline function and the global estimates of enzyme activity were calculated using the "raster" package (Hijmans, 2020). The estimates of enzyme activity for 2081 to 2100 is presented as the average of the results for the eight models for each SSP scenario at each depth. These steps were performed in R v. 4.0.3 (R Core Team, 2020).

These estimates of enzyme activity were used to display the changes in the C:N, C:P, and N:P flow ratios (calculation details in Section 2.2) at the three depths of interest. To understand the effect of temperature on the flow ratios, we computed their percent relative change in 2081 to 2100 compared with 1970 to 2000 for the

two SSP scenarios. The calculation for the flow ratios also used the "raster" package (Hijmans, 2020) in R v. 4.0.3 (R Core Team, 2020).

## 2.2 | Calculation of the flow ratio of liberated resources

Combining previously published purified kinetics data BGase and NAGase (Min et al., 2014) with the newly-generated APase data set (Appendix A in Supporting Information; Section 2.3) allowed us to describe the relative release rates at which C and P, and N and P, are cleaved from the MUB-labeled substrates via these enzymes' activities by calculating flow ratios of the liberated resources (Billings & Ballantyne, 2013; Min et al., 2014). As the substrates used for BGase, NAGase, and APase are proxies for cellulose, chitin (German et al., 2012; Sinsabaugh et al., 2008), and phosphomonoesters (Sinsabaugh et al., 2008), respectively, we converted the units of fluorescence from the purified enzyme experiment into numbers of C, N (Lehmeier et al., 2013), and P atoms released during each enzyme-promoted decay reaction. The cleaving of these respective substrates is comparable with the release of one glucose, one N-Acetylglucosamine, and one phosphate molecule. Thus, the C:P flow ratio resulting from one decay transaction of each of these reactions would release six atoms of C for every one atom of P, and the corresponding N:P flow ratio would release one N for every one P atom. Flow ratios from the estimated enzyme activity for each temperature ( $T$ ) were calculated as:

$$\frac{dC}{dP} = \frac{V_{\text{maxBGase}}(T)}{V_{\text{maxAPase}}(T)} \times 6 \quad (2)$$

$$\frac{dN}{dP} = \frac{V_{\text{maxNAGase}}(T)}{V_{\text{maxAPase}}(T)} \quad (3)$$

where  $V_{\text{maxBGase}}$ ,  $V_{\text{maxNAGase}}$ , and  $V_{\text{maxAPase}}$  are estimates of the maximum rate of reaction obtained from the general linear model using the Arrhenius-transformed specific enzyme activity (see Section 2.1). The C:N flow ratio was calculated in a similar manner, as described in Lehmeier et al. (2013) and Min et al. (2014).

## 2.3 | Calculation of the acid phosphatase specific activity and temperature sensitivity ( $E_a$ )

We calculated the specific activity of the APase enzyme (Appendix A in Supporting Information) using a modified version of the approach described in DeForest (2009). Because the specific activities were recorded when neither substrate nor enzyme was limiting, we interpret the observed rates as intrinsic specific activities. We note that relative to exoenzyme activities reported using soil slurries (e.g., German et al., 2012), the experimental conditions for the current study promote the interaction of enzyme and substrate because of the absence of soil particles whose

adsorption capacity can limit enzyme catalysis (Conant et al., 2011; Quiquampoix, 2000). Similarly, we interpret estimates of temperature sensitivity as intrinsic temperature sensitivities of the enzyme.

## 2.4 | Statistical analyses

We used a non-parametric approach—quantile regression—to estimate conditional medians of the specific activity of APase at different pH and temperature. The non-parametric approach was necessary because the data did not meet the assumptions of normality and homoscedasticity even after multiple transformations. The models predicted APase activity as a function of pH, temperature, and their interaction. We assessed their statistical significance using a Wald test. Both approaches were performed using the “quantreg” package (Koenker, 2021).

To compare temperature sensitivities across the three enzymes, we generated likelihood ratios from the APase kinetics, comparing the full model likelihood to the nested model likelihood. We determined the statistical significance of each pH on  $E_a$  of APase by testing the pairwise differences between  $E_a$  at different pH. We created the matrices for each model separately before fitting a linear model to calculate the log-likelihoods. We assessed these analyses in conjunction with the analogs presented for BGase and NAGase in Min et al. (2014; Appendix B in Supporting Information).

All statistical analyses were performed using R v. 4.0.3 (R Core Team, 2020) and the results were considered significant when  $p < .05$ .

## 3 | RESULTS

The C:P and N:P flow ratios contrasted with previously published with C:N flow ratios (Min et al., 2014; Figure 1a). APase responses to temperature and pH prompted consistent, warming-induced increases in the estimated flow ratios of C:P (Figure 1b) and N:P (Figure 1c) across pH, with the largest range expressed by the C:P estimates. Greater differences between experimental temperatures were observed at pH 6.5 for estimated C:P and N:P flow ratios. These results were driven by the stronger effect of warming on the specific activity of APase in more acidic conditions, at and below pH 4.5 (Figure 2), in contrast to the increased responsiveness of BGase and NAGase to warming at and above pH 5.5 (Min et al., 2014). Changes in flow ratios reflect differences in  $E_a$  values between enzymes (Table 1; Figure 3). Min et al. (2014) demonstrated that the temperature sensitivity of BGase trends downward as pH approaches near-neutral values, and NAGase exhibits somewhat variable behavior across the same pH range. In contrast, APase showed the lowest temperature sensitivity at pH 6.5, and the highest temperature sensitivities at the most extreme pH assayed. APase displayed the greatest  $E_a$  variation at pH 7.5, with a standard deviation of  $8.29 \text{ kJ mol}^{-1}$  (Figure 3).

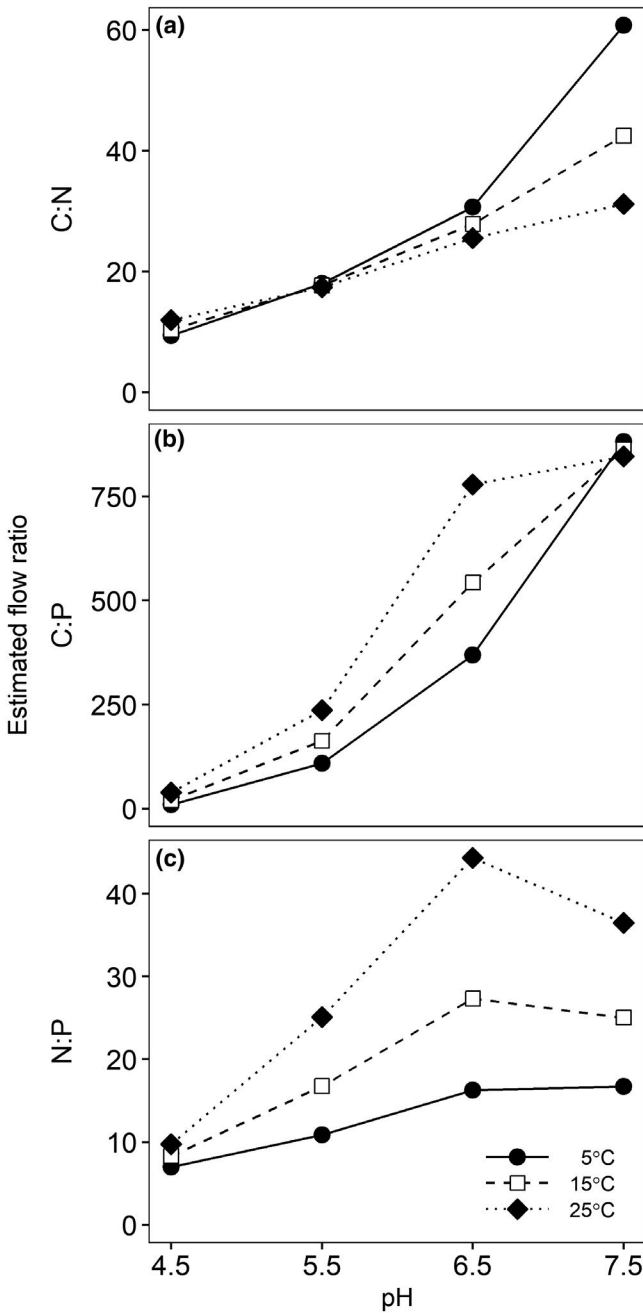


**FIGURE 1** Estimated flow ratio of liberated resources from enzyme activity. (a) Estimated C:N flow ratio from BGase and NAGase activity. (b) Estimated C:P flow ratio from BGase and APase activity. (c) Estimated N:P flow ratio from NAGase and APase activity. Values for C and N release rates from enzyme activity are derived from Min et al. (2014)

Global-scale projections of BGase, NAGase, and APase activity reflect the exoenzymes' variabilities in  $E_a$  across the pH range, as estimated by the spline function (Figure 3). APase  $E_a$  varied less between pH 4.5 and 5.2, exhibiting standard variation of 2.1 and  $2.2 \text{ kJ mol}^{-1}$  in that interval. Standard deviation was greater at pH values above 6.9, reaching up to  $8.3 \text{ kJ mol}^{-1}$  at pH 7.5. APase  $E_a$  across the pH range was consistently lower than the  $E_a$  of the other two enzymes, except at pH 7.5 in comparison with BGase (Table 1).

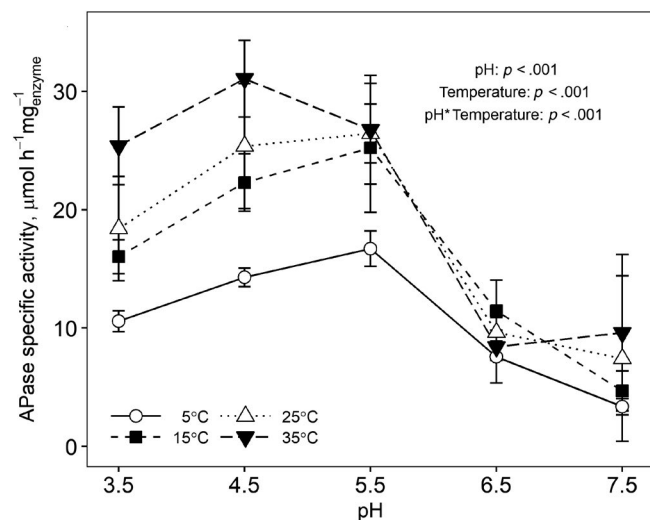


FIGURE 2 Specific activity of APase at different temperatures as a function of pH. Each point is the mean of six replicates; error bars reflect one standard deviation from the mean

TABLE 1 Activation energy ( $E_a$ ,  $\text{kJ mol}^{-1}$ ) values for BGase, NAGase, and APase across a common pH interval

	pH 4.5	pH 5.5	pH 6.5	pH 7.5
BGase	65.18 <sup>A,a</sup>	37.25 <sup>B,a</sup>	27.99 <sup>BC,a</sup>	16.91 <sup>C,a</sup>
NAGase	28.91 <sup>A,b</sup>	39.40 <sup>A,a</sup>	36.78 <sup>A,a</sup>	45.23 <sup>A,b</sup>
APase	17.43 <sup>A,c</sup>	10.52 <sup>ABC,b</sup>	2.27 <sup>BC,b</sup>	18.32 <sup>AC,a</sup>

Note: Upper case letters denote significant differences in  $E_a$  across pH values for a given enzyme; lower case letters denote significant differences in  $E_a$  between two enzymes at a given pH (see Appendix B in Supporting Information for a detailed explanation of the statistical approach). BGase and NAGase data originally reported in Min et al. (2014).

In contrast, BGase and NAGase data derived from Min et al. (2014) exhibited the greatest variability of  $E_a$  close to pH 4.5, exhibiting standard deviations up to 8.1 and 5.6  $\text{kJ mol}^{-1}$ , respectively, though NAGase  $E_a$  also exhibited a large standard deviation of 5.4  $\text{kJ mol}^{-1}$  at pH 6.7. Note that global scale projections employ spline-function derived enzyme activities based on pH values that can differ from the laboratory experiments, generating continuous functions of  $E_a$  as it varies with pH (Figure 3).

Projecting  $E_a$  of the three enzymes as they vary across soil pH at the global scale revealed depth-dependent, region-specific changes in the three flow ratios with warming. Each flow ratio's projected change reflects the  $E_a$  of the enzymes comprising it. The SSP2-4.5 scenario, in which globally averaged temperatures are expected to increase by  $3.3^\circ\text{C}$  by 2100, results in maximum projected increases in C:N, C:P, and N:P flow ratios of 6.3%, 75.4%, and 107.5% at the soil surface (Figures 4a, 5a and 6a). These values almost double for the C:N, C:P, and N:P flow ratios under SSP5-8.5, which predicts temperatures rising by  $5.5^\circ\text{C}$ , with maximum projected increases reaching up to 12.9%,

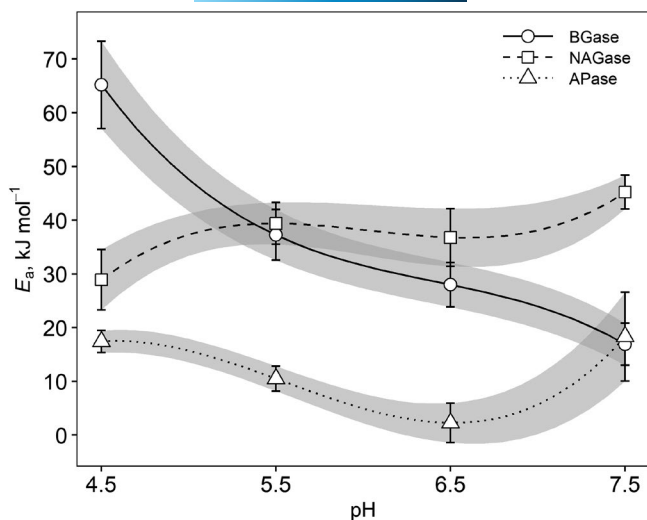
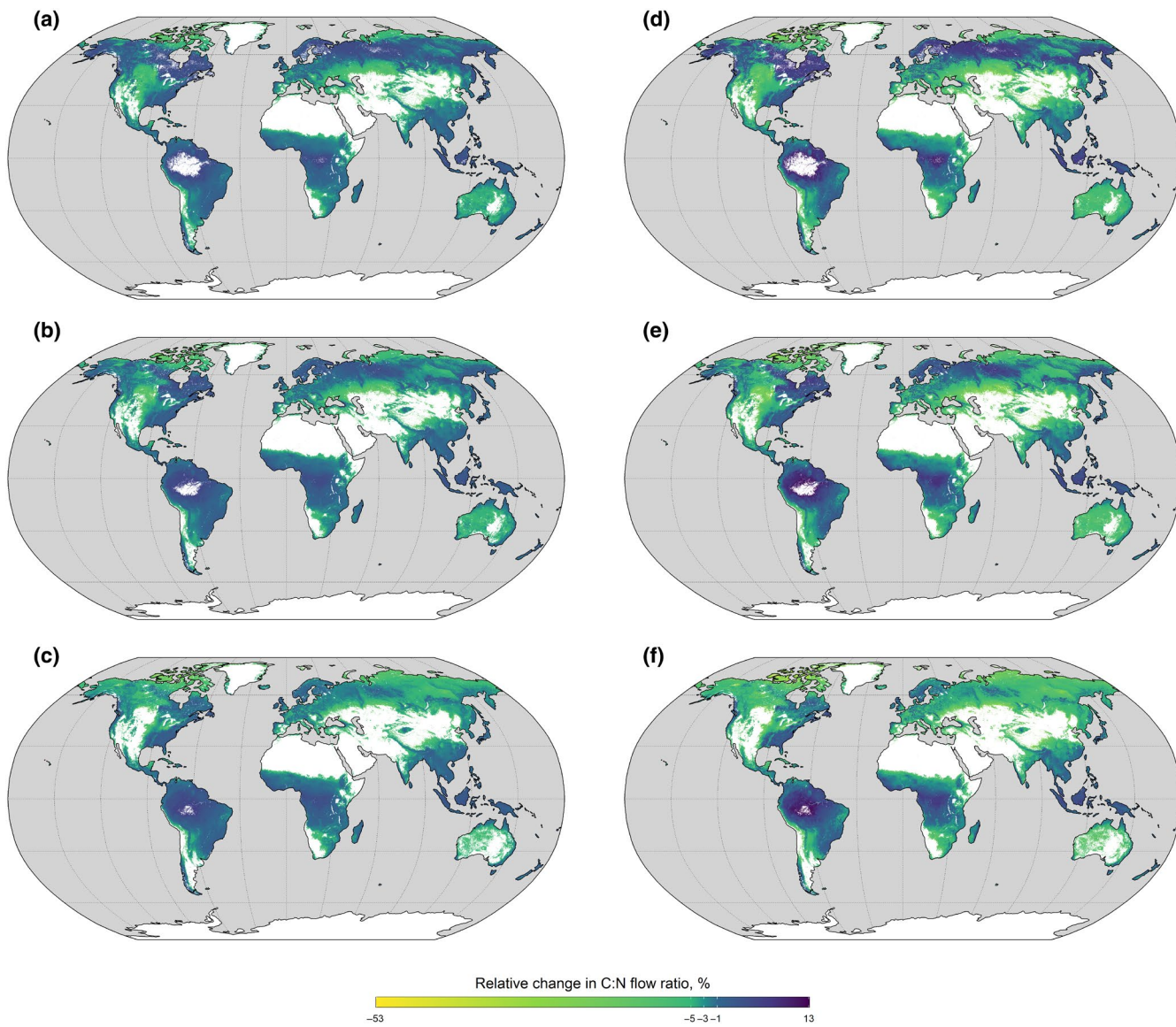


FIGURE 3 Variation in temperature sensitivity (expressed as  $E_a$ ) for pH between 4.5 and 7.5 for APase, BGase, and NAGase. Points and error bars represent the measured average and one standard deviation of the temperature sensitivity for each enzyme. Lines and shaded areas correspond to the estimated average and one standard deviation of  $E_a$  across the pH range, derived from a spline function (see Section 2.1 for details). BGase and NAGase data derived from Min et al. (2014)

155.1%, and 161.2%, respectively (Figures 4d, 5d, and 6d). In contrast to the maximum projected increases, the predicted average global-scale change of all flow ratios is much smaller. The C:N, C:P, and N:P flow ratios exhibit average projected changes at the soil surface of -1.9%, 18.9%, and 19.9%, respectively, for SSP2-4.5, and -3.1%, 35.7%, and 37.7% for SSP5-8.5 (Table S2). Analogous, average projected changes at 1 m were approximately -3.5%, 17.1%, and 22.7% for SSP2-4.5 and -5.7%, 31.7%, and 43.2% for SSP5-8.5 (Table S2). For C:P and N:P flow ratios, up to 46% of the area analyzed globally at all depths is projected to experience above average changes in these three flow ratios. Note that the global area across which flow ratios are projected is greater in surface soils and at 30 cm depth compared with 1 m depth because a smaller area exhibits soil pH between 4.5 and 7.5 at 1 m; approximately 75.9%, 76.1%, and 70.3% of Earth's land area falls within this pH range at 0, 30, and 100 cm (calculated from Hengl et al., 2017).

No region exhibited a decline in the N:P flow ratio, and 2% of the land surface area experienced a decline in C:P flow ratio in both SSP scenarios. In contrast, declines in C:N flow ratios were observed across 63%–85% of the terrestrial landscape from 0 to 100 cm in both SSP scenarios. Areas of increasing C:N flows decreased with depth to 25.9% of the soil area at 30 cm (Figure 4b,e), and to 15.6% of the soil area at 100 cm in both scenarios (Figure 4c,f). Relatively greater increases in temperature at higher latitudes resulted in greater flow ratio increases for C:P and N:P in these regions (Figures 5 and 6). Increases in NAGase  $E_a$  above pH 5.5 (Figure 3) promoted declining C:N flow ratios with warming across much of the globe.



**FIGURE 4** Relative change in C:N flow ratio from 1970–2000 to 2081–2100 for SSP2-4.5 at (a) 0 cm, (b) 30 cm, and (c) 100 cm of depth, and for SSP5-8.5 at (d) 0 cm, (e) 30 cm, and (f) 100 cm of depth, reflecting the activities of  $\beta$ -glucosidase and N-acetyl-Glucosaminidase (derived from Min et al., 2014). See text for explanation of flow ratio concept. Values in the color bar represent the minimum, the average minus two standard deviations, the average, the average plus two standard deviations, and the maximum relative change in the C:N flow ratio, respectively

## 4 | DISCUSSION

Understanding the intrinsic temperature response of exoenzymes with varying pH allows us to investigate the potential change in the relative rate of liberation of different organic resources as environmental conditions change. Our work demonstrates that pH and temperature exert a meaningful, interactive effect on the specific activity of APase in ways different from those previously observed for BGase and NAGase (Min et al., 2014), and that this feature is reflected in the degree of change in the C:P and N:P flow ratios across soil pH and temperatures. We cannot use these results to predict the bioavailability of C, N, and P resources that are derived from a tremendous diversity of processes in any given soil; rather, they offer

proof-of-concept that the interaction between pH and temperature sensitivities of SOM decay reactions can help shape soil provision of needed resources to biota by modulating stoichiometric constraints.

### 4.1 | Flow ratios of resources liberated from enzymatic activity

The differences in estimated flow ratios of C:N, C:P, and N:P with varying pH and temperature (Figure 1) highlight the importance of understanding temperature sensitivities of different exoenzymes that release important resources for soil microbes and vegetation as environmental conditions vary. Because phosphatase enzymes

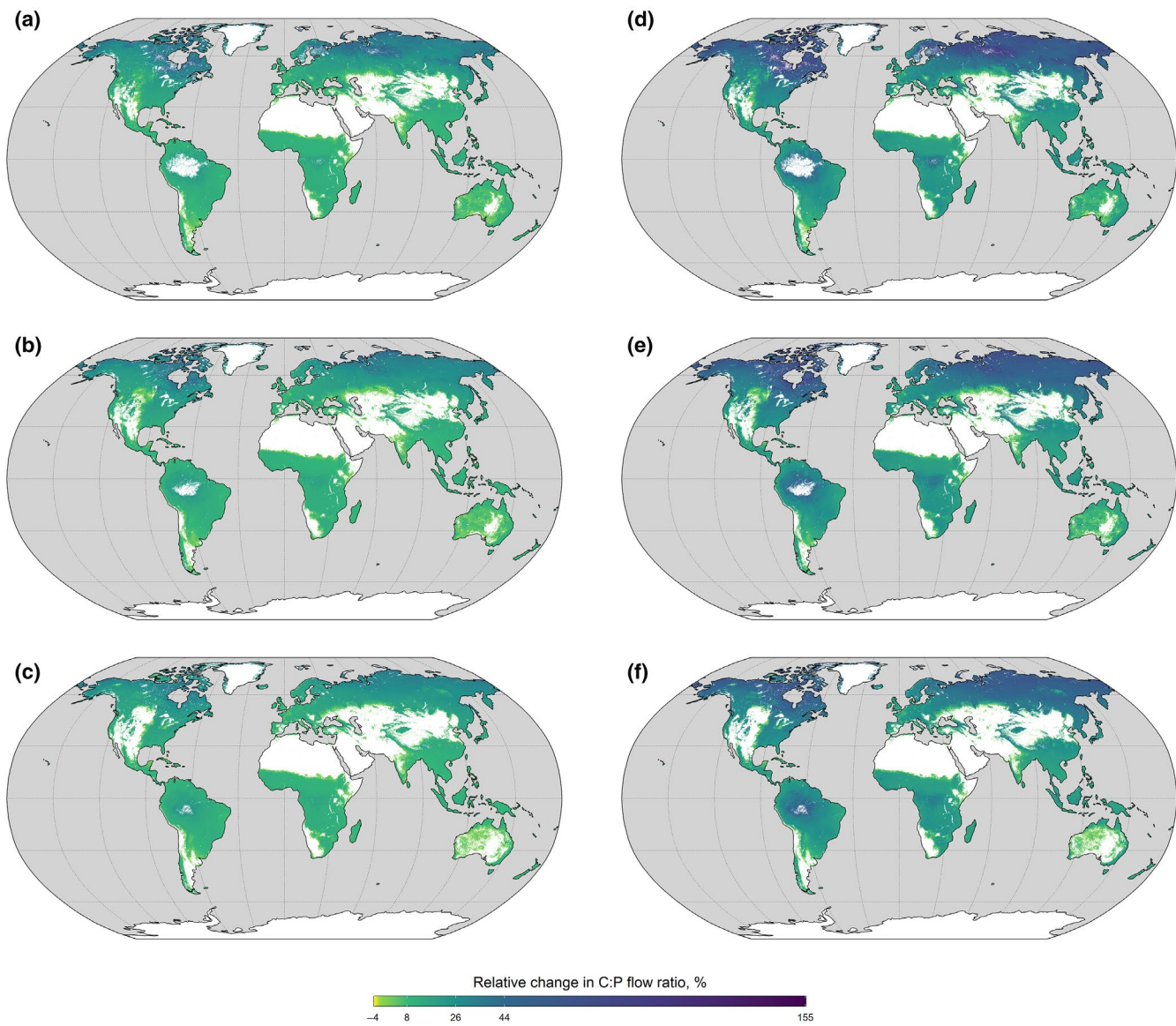


**FIGURE 5** Relative change in C:P flow ratio from 1970–2000 to 2081–2100 for SSP2-4.5 at (a) 0 cm, (b) 30 cm, and (c) 100 cm of depth, and for SSP5-8.5 at (d) 0 cm, (e) 30 cm, and (f) 100 cm of depth, reflecting the activities of  $\beta$ -glucosidase (derived from Min et al., 2014) and acid phosphatase (this study). See text for explanation of flow ratio concept. Values in the color bar represent the minimum, the average minus two standard deviations, the average, the average plus two standard deviations, and the maximum relative change in the C:P flow ratio, respectively

are the main mechanism responsible for the mineralization of soil organic P (Condron et al., 2005), a process especially important in ecosystems as P availability from dissolution of primary minerals wanes with soil age (Walker & Syers, 1976), their response to temperature and pH relative to agents of C and N release such as BGase and NAGase may be an important influence on the stoichiometry of bioavailable resources. A disproportionate response of one exoenzyme to temperature at a given pH relative to another could trigger a stoichiometric imbalance with warming (here, among C, N, and P resources; Cleveland & Liptzin, 2007). Changes in the degree to which resources become available in the soil may affect microbes' nutrient acquisition strategies (Billings & Ballantyne, 2013), prompt microbial adaptation under different environmental conditions (Bradford,

2013) to reestablish homeostasis, or promote changes in the vegetation's response to nutrient limitation (Du et al., 2020; Farnier et al., 2013; Hou et al., 2020). Considering the often-large role of microbial biomass P in total soil organic P stocks, especially in highly weathered soils where it can amount to almost 90% of that pool (Brookes et al., 1984; Condron et al., 2005), microbial responses to changing resource availability could trigger changes in the proportion of total soil P derived from microbial versus plant material. Our results suggest that the degree to which P limitation may be enhanced or mitigated as other nutrients become more or less available can vary significantly with temperature and pH, with pH serving as a master variable dictating the temperature responses of key features of SOM decay.

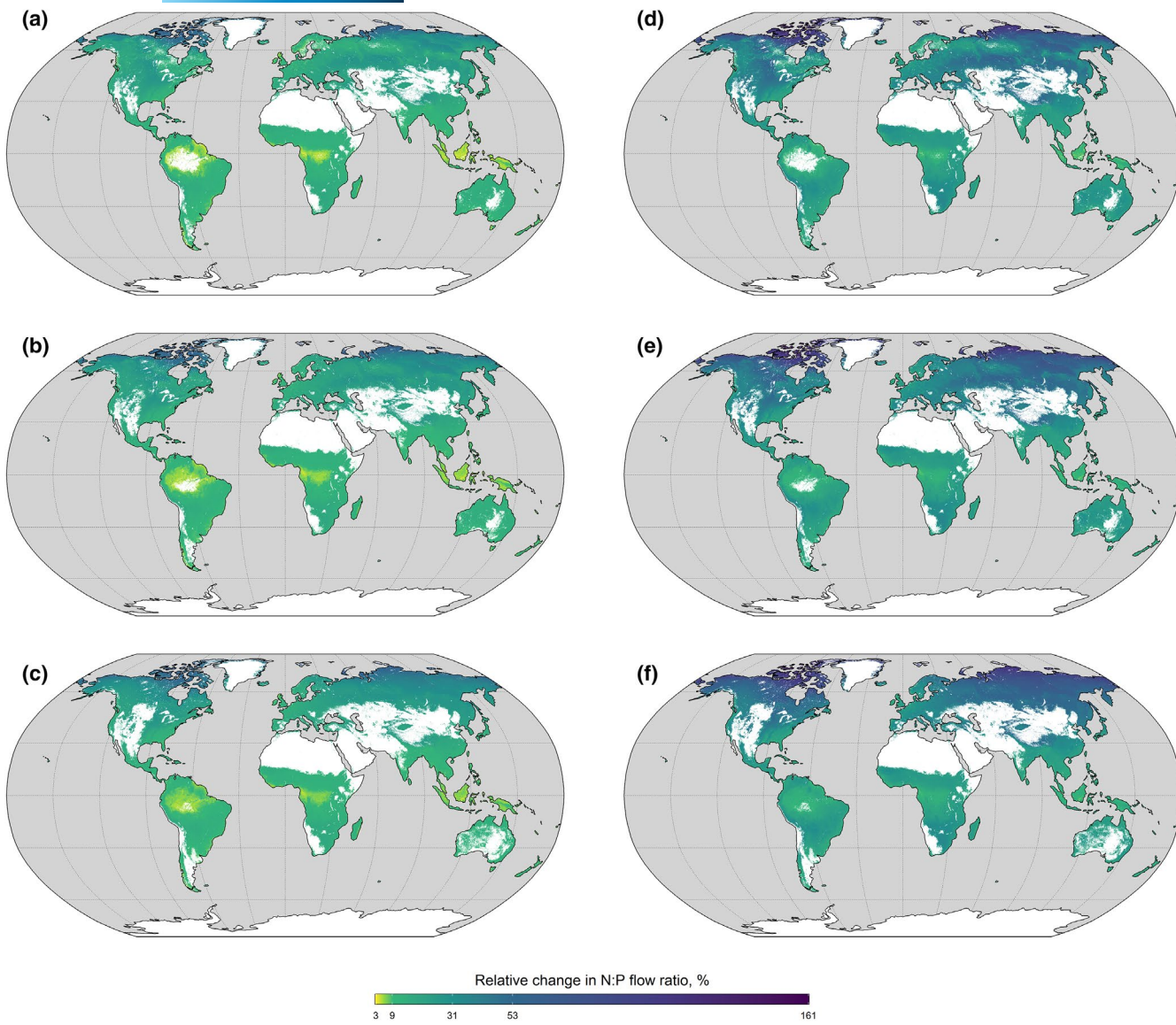


**FIGURE 6** Relative change in N:P flow ratio from 1970–2000 to 2081–2100 for SSP2-4.5 at (a) 0 cm, (b) 30 cm, and (c) 100 cm of depth, and for SSP5-8.5 at (d) 0 cm, (e) 30 cm, and (f) 100 cm of depth, reflecting the activities of N-acetyl-Glucosaminidase (derived from Min et al., 2014) and acid phosphatase (this study). See text for explanation of flow ratio concept. Values in the color bar represent the minimum, the average minus two standard deviations, the average, the average plus two standard deviations, and the maximum relative change in the N:P flow ratio, respectively

The increasing C:P and N:P flow ratios with warming exhibited here (Figure 1b,c) are consistent with warming effects reported for environmental samples (Dijkstra et al., 2012; Sardans et al., 2012; Yue et al., 2017); our work demonstrates that pH can dictate the magnitude of these effects. The work further indicates that these effects are evident even when the soil medium and microbes themselves are absent, demonstrating fundamental, biochemical responses to environmental conditions. Variations in the C:P flow ratio, for example, were minimal at pH 7.5 and greatest at pH 4.5 with rising temperatures (Figure S2). Consistently low APase activity at pH 7.5 at all temperatures (Figure 2) relative to the higher BGase activity at the same pH (Min et al., 2014) led to less variation in the flow ratio with warming at that pH, whereas the opposite happened

at pH 4.5, where APase functions close to its known pH optimum. The difference in the relative rates of enzyme activity for BGase and APase also explains the range of the C:P flow ratio values across the pH gradient, especially as they are much higher at pH values near neutral. Similar patterns for the N:P flow ratio can be explained by the same reasoning. Moreover, the pH values at which variation of C:P and N:P flow ratios were at their lowest were also the pH values at which temperature sensitivities were more comparable for the enzymes (Table 1). Of course, these results cannot provide accurate projections of the stoichiometry of all resources liberated into bioavailable forms throughout soil profiles in the future, nor can they accurately depict bioavailable C, N, and P as decay proceeds. Instead, this work highlights the power of temperature and pH as interactive

determinants of changing relative availabilities of biotic resources in soil, and demonstrates the capacity of well-characterized enzyme kinetics to serve as constraints on those projections.

To the best of our knowledge, APase dynamics have not been explored across ecologically relevant pH and temperature gradients. As a result, we needed to characterize the APase kinetics to estimate the change in flow ratios. We report similar pH optima for APase activity as those reported in studies of environmental samples (Hui et al., 2013), as well as one employing isolated mycelial mats of ectomycorrhizal fungi (Antibus et al., 1986). We further report a positive influence of temperature on APase activity within the range tested, as might be expected given extensive documentation of increasing temperature promoting activity of enzymes isolated in purified buffer (Min et al., 2014) and environmental samples (German et al., 2012; Koch et al., 2007; Min et al., 2019; Wallenstein et al., 2010), including APase (Hui et al., 2013; Margalef et al., 2017). Both pH and temperature can promote changes in enzyme conformation, modifying accessibility of active sites and the stability of its own structure (Wallenstein et al., 2010), at least partially explaining why their interaction was significant for APase. Indeed, adsorption of multiple enzymes onto soil surfaces varies with pH and affects enzyme catalytic activity (Rao et al., 2000) and can even increase the pH optimum (Leprince & Quiquampoix, 1996). These changes in the catalytic power of enzymes are related to the protein folding processes that respond to pH through changes in the isoelectric point of the enzyme (Leprince & Quiquampoix, 1996; Quiquampoix, 2000) and to temperature through the thermal stability of the protein structure (Bradford, 2013; Wallenstein et al., 2010). Nonetheless, it remains unclear why individual pairs of enzymes and relevant substrates exhibit unique responses to pH and temperature.

Our investigation of the influence of pH on the  $E_a$  of APase allows us to explore the interaction of pH and temperature on the activity of this enzyme and to compare these effects to those reported for BGase and NAGase. The temperature sensitivity estimates for APase reported here are lower than those observed in environmental samples (Bárta et al., 2014; Blagodatskaya et al., 2016; Hui et al., 2013; Razavi et al., 2017). Because we characterized APase kinetics in a purified setting, the discrepancies between the temperature sensitivities reported here and those reported for environmental samples likely reflect some combination of edaphic modification of enzyme activity, and the response of microbes to temperature. Such influences are absent from the data reported here, illuminating fundamental biochemical properties of APase. Specifically, our results highlight how increasing temperatures promote higher P release rates during OM decay at relatively low pH, but to a lesser degree at pH values closer to neutral (Figure 2). Furthermore, relatively enhanced variation in APase temperature sensitivity at pH 6.5 and 7.5 (Figure 3) reduces our capacity to predict APase-promoted P availability as temperature varies. Still, these differences in APase temperature sensitivity most probably drive the changes in the N:P flow ratio (Figure 1c), given that NAGase does not exhibit significant variation in response to temperature across the pH range (Min et al., 2014; Table 1). Conversely, the estimated C:P flow ratio (Figure 1b)

results from the differential effects of increasing temperatures on both BGase and APase activity (Table 1).

## 4.2 | Global-scale projections of C:N, C:P, and N flow ratios

Spatially explicit representations of the biochemical limitations on the release of C, N, and P by activities of BGase (C), NAGase (N and C), and APase (P) with warming at different pH allow us to forecast the potential importance of changes in these fluxes under different climate scenarios relative to historical temperatures. This approach assumes that the rate at which subsoils experience warming to be similar to that of surface soils (Hicks Pries et al., 2017). The geographical patterns and depth trends for the relative change in the flow ratios track the different response of the enzyme's temperature sensitivity to the pH. As a result, global projections show a mostly positive relationship of the C:P flow ratio with warming (Figure 5), whereas the N:P flow ratio exhibits an exclusively positive change globally with rising temperatures, regardless of soil pH (Figure 6). Less than 3% of the area projected to exhibit the lowest relative change in the C:P flow ratio with rising temperatures in both SSP scenarios is associated with pH 7.5 (Figure 1b), where the temperature sensitivity of BGase is similar to that of APase (Table 1). In contrast, an overall neutral to negative relationship was observed for the C:N flow ratio with warming globally (Figure 4). Projected changes in the N:P and the C:N flow ratios reflect the overall higher temperature sensitivity of NAGase across the studied pH gradient (Figure 3). Because NAGase is more sensitive to warming than APase across the acidic to neutral pH gradient, the relative change in projected N:P flow ratios are solely positive. Areas of strongly acidic pH values (<5.5) exhibit positive changes in the C:N flow ratio with rising temperatures, but the differences are most substantial at pH 7.5 (Figures 1a and 3). This feature explains why the expected average change in the C:N flow ratio is between 0% and -5% in both SSP scenarios (Figure 4; Table S2) as soils with pH between 7.0 and 7.5 correspond to approximately 11% of the total soil area at all depths. The total area with above-average changes for the three flow ratios is similar across depths under the two SSPs. Thus, although all enzyme reactions in a given grid cell are examined under the same projected temperature increases, C:P, N:P, and C:N flow ratios exhibit different temperature responses due to the strong effect of soil pH on enzyme temperature sensitivities.

Regional differences in projected flow ratios reflected these relative differences in exoenzyme activities. We observed greater relative changes in C:N, C:P, and N:P flow ratios in the Arctic at all depths relative to current climate conditions, although the estimated change depended on the enzyme pair (Figures 4–6). This is consistent with the greater degree of warming prescribed in higher latitude regions in both SSP scenarios and the predominance of soil pH values below 6 in those regions that favor the activity of all three enzymes. Conversely, generally acidic, highly weathered tropical soils did not exhibit as much change in flow ratios by the end of

the century due to their relatively small increases in temperature. Consistent with the possible future enhancement of P limitation in the tropics and the Arctic that the C:P flow ratio hints at (Figure 5), projections for both C:N and N:P flow ratios (Figures 4 and 6) suggest that predominantly N-limited areas, especially in the northern temperate zone, may experience relatively greater availability of organically-derived N as temperatures rise. However, though increased N availability can shift systems towards P limitation (Chen et al., 2020; Li et al., 2016; Penuelas et al., 2013), greater availability of N can also increase APase activity and P cycling rates (Marklein & Houlton, 2012; Olander & Vitousek, 2000). It remains unclear how these mechanisms will proceed in regions already experiencing N- or P-limitation (Chen et al., 2020; Du et al., 2020; Farnier et al., 2013; Hou et al., 2021).

We note that these model projections assume no change in stoichiometry of SOM inputs, precipitation, or nutrient availability derived from sources other than these exoenzymes activities. All these features are likely to change in the future, with probable consequences for the stoichiometry of bioavailable resources. Elevated CO<sub>2</sub> (eCO<sub>2</sub>), for example, generally has a positive impact on plant and soil C:P and C:N ratios (Luo et al., 2006; Sardans et al., 2012). Although NAGase can respond positively to an increase in CO<sub>2</sub> concentrations (Kelley et al., 2011), the effect on multiple other enzymes' activities appears negligible (Kelley et al., 2011; Xiao et al., 2018). Additionally, changes in soil microbial communities with eCO<sub>2</sub> can shift fungi:bacteria ratios (Castro et al., 2010) and in turn affect enzyme production (Kelley et al., 2011) and their stoichiometric balance, possibly leading to altered rates of OM decomposition at surface and in the subsurface. Soil moisture variability also can affect microbial resource allocation and consequent enzyme production (Manzoni et al., 2016; Steinweg, Dukes et al., 2013), further affecting microbial composition as physiological stress can trigger changes in nutrient demand (Schimel et al., 2007; Tiemann & Billings, 2011). Nutrient availability from sources other than SOM decay, and from the activities of exoenzymes other than those examined here, represents another feature of terrestrial ecosystems likely to modify soil enzyme activities in the coming decades. Nitrogen deposition, for example, can have a positive effect on APase activity (Marklein & Houlton, 2012), and can also shift fungal communities and affect plant acquisition of P, possibly constraining productivity in P-limited systems (Treseder et al., 2018). Similarly, increased P inputs often suppress APase activity (Marklein & Houlton, 2012; Olander & Vitousek, 2000). Although the current work does not explicitly address these factors, it provides a starting point for developing testable hypotheses probing how edaphic resources for biotic uptake may change in a changing climate.

## 5 | CONCLUSIONS

Parsing out the intrinsic biochemical responses of soil exoenzymes is a valuable tool for the modeling community. From such data, we cannot hope to accurately project ecosystem nutrient limitation; a

diversity of enzymes provides liberated resources to biota in most soils (German et al., 2011; Sinsabaugh et al., 2008), and nutrients are also provided by mineral weathering (Vitousek et al., 2010; Walker & Syers, 1976) and atmospheric inputs (Galloway et al., 2008; Mahowald et al., 2008; Vitousek et al., 2010). Rather, intrinsic exoenzyme kinetics provide the basis to constrain future ecosystem nutrient limitation. All else equal, modified flow ratios as temperature and pH change could lead ecosystems to experience changes in the identity of limiting nutrients. Results from this work examining a small subset of the exoenzymes common in soils globally suggest that warming could prompt bioavailability of resources derived from those exoenzymes to shift from N- to P-limitation with warming due to relatively small enhancements of P release from decaying organic matter with warming. The spatially explicit global maps presented here thus do not aim to provide a projection of in situ flow ratios. Rather, they demonstrate proof-of-concept that the differential effects of temperature and pH on globally-important mechanisms driving the release of C and nutrients from SOM can result in shifting stoichiometries of bioavailable resources for soil microbes and vegetation. Concerns of anthropogenic climate change motivate many studies of the effects of temperature on soil processes; our work highlights the importance of the interaction of temperature and soil pH at diverse spatial scales for forecasting bioavailable resources in a changing climate. This interaction can dictate differential rates at which organically bound biotic resources are liberated, and thus the responses of biota to climate change.

## ACKNOWLEDGMENTS

We acknowledge the World Climate Research Programme, which, through its Working Group on Coupled Modelling, coordinated and promoted CMIP6. We thank the climate modeling groups for producing and making available their model output, the Earth System Grid Federation (ESGF) for archiving the data and providing access, and the multiple funding agencies who support CMIP6 and ESGF. We thank Dexter White for laboratory assistance, Dr. Daniel Reuman for motivating the log-likelihood analysis, and an anonymous reviewer for helpful comments on the manuscript. This material is based upon work supported by the National Science Foundation under Award N°. OIA-1656006 and matching support from the State of Kansas through the Kansas Board of Regents. Support was also provided by NSF EAR-2026874, USDA NIFA 2021-67019-34338, and the University of Kansas Field Station student grant program.

## CONFLICT OF INTEREST

The authors have no conflict of interest to declare.

## DATA AVAILABILITY STATEMENT

The data that support the findings of this study are available in Zenodo at <https://doi.org/10.5281/zenodo.5651104>.

## ORCID

Ligia F. T. de Souza  <https://orcid.org/0000-0002-3925-6383>

Sharon A. Billings  <https://orcid.org/0000-0003-1611-526X>

## REFERENCES

Antibus, R. K., Kroehler, C. J., & Linkins, A. E. (1986). The effects of external pH, temperature, and substrate concentration on acid phosphatase activity of ectomycorrhizal fungi. *Canadian Journal of Botany*, 64, 2383–2387. <https://doi.org/10.1139/b86-315>

Arrhenius, S. (1889). Über die Reaktionsgeschwindigkeit bei der Inversion von Rohrzucker durch Säuren. *Zeitschrift für Physik Chemie*, 4, 226–248. <https://doi.org/10.1515/zpch-1889-0416>

Bárta, J., Šlajsová, P., Tahovská, K., Picek, T., & Šantrůčková, H. (2014). Different temperature sensitivity and kinetics of soil enzymes indicate seasonal shifts in C, N and P nutrient stoichiometry in acid forest soil. *Biogeochemistry*, 117, 525–537. <https://doi.org/10.1007/s10533-013-9898-1>

Berthrong, S. T., Jobbágy, E. G., & Jackson, R. B. (2009). A global meta-analysis of soil exchangeable cations, pH, carbon, and nitrogen with afforestation. *Ecological Applications*, 19, 2228–2241. <https://doi.org/10.1890/08-1730.1>

Billings, S. A., & Ballantyne, F. T. (2013). How interactions between microbial resource demands, soil organic matter stoichiometry, and substrate reactivity determine the direction and magnitude of soil respiratory responses to warming. *Global Change Biology*, 19, 90–102. <https://doi.org/10.1111/gcb.12029>

Blagodatskaya, E., Blagodatsky, S., Khomyakov, N., Myachina, O., & Kuzyakov, Y. (2016). Temperature sensitivity and enzymatic mechanisms of soil organic matter decomposition along an altitudinal gradient on Mount Kilimanjaro. *Scientific Reports*, 6, 1–11. <https://doi.org/10.1038/srep22240>

Bradford, M. A. (2013). Thermal adaptation of decomposer communities in warming soils. *Frontiers in Microbiology*, 4, 1–16. <https://doi.org/10.3389/fmicb.2013.00333>

Bradford, M. A., Davies, C. A., Frey, S. D., Maddox, T. R., Melillo, J. M., Mohan, J. E., Reynolds, J. F., Treseder, K. K., & Wallenstein, M. D. (2008). Thermal adaptation of soil microbial respiration to elevated temperature. *Ecology Letters*, 11, 1316–1327. <https://doi.org/10.1111/j.1461-0248.2008.01251.x>

Brookes, P. C., Powlson, D. S., & Jenkinson, D. S. (1984). Phosphorus in the soil microbial biomass. *Soil Biology and Biochemistry*, 16, 169–175. [https://doi.org/10.1016/0038-0717\(84\)90108-1](https://doi.org/10.1016/0038-0717(84)90108-1)

Castro, H. F., Classen, A. T., Austin, E. E., Norby, R. J., & Schadt, C. W. (2010). Soil microbial community responses to multiple experimental climate change drivers. *Applied and Environmental Microbiology*, 76, 999–1007. <https://doi.org/10.1128/AEM.02874-09>

Chen, J., van Groenigen, K. J., Hungate, B. A., Terrer, C., van Groenigen, J. W., Maestre, F. T., Ying, S. C., Luo, Y., Jorgensen, U., Sinsabaugh, R. L., Olesen, J. E., & Elsgaard, L. (2020). Long-term nitrogen loading alleviates phosphorus limitation in terrestrial ecosystems. *Global Change Biology*, 26, 5077–5086. <https://doi.org/10.1111/gcb.15218>

Christopoulos, D. T. (2019). Inflection: Finds the inflection point of a curve. R package version 1.3.5. <https://CRAN.R-project.org/package=inflection>

Cleveland, C. C., & Liptzin, D. (2007). C:N:P stoichiometry in soil: Is there a “Redfield ratio” for the microbial biomass? *Biogeochemistry*, 85, 235–252. <https://doi.org/10.1007/s10533-007-9132-0>

Conant, R. T., Ryan, M. G., Ågren, G. I., Birge, H. E., Davidson, E. A., Eliasson, P. E., Evans, S. E., Frey, S. D., Giardina, C. P., Hopkins, F. M., Hyvönen, R., Kirschbaum, M. U. F., Lavallee, J. M., Leifeld, J., Parton, W. J., Megan Steinweg, J., Wallenstein, M. D., Martin Wetterstedt, J. Å., & Bradford, M. A. (2011). Temperature and soil organic matter decomposition rates—Synthesis of current knowledge and a way forward. *Global Change Biology*, 17, 3392–3404. <https://doi.org/10.1111/j.1365-2486.2011.02496.x>

Condron, L. M., Turner, B. L., & Cade-Menun, B. J. (2005). Chemistry and dynamics of soil organic phosphorus. In T. Sims & A. N. Sharpley (Eds.), *Phosphorus: Agriculture and the environment*. Agronomy

monographs (Vol. 46, pp. 87–121). ASA, CSA, and SSSA. <https://doi.org/10.2134/agronmonogr46.c4>

Davidson, E. A., & Janssens, I. A. (2006). Temperature sensitivity of soil carbon decomposition and feedbacks to climate change. *Nature*, 440, 165–173. <https://doi.org/10.1038/nature04514>

DeForest, J. L. (2009). The influence of time, storage temperature, and substrate age on potential soil enzyme activity in acidic forest soils using MUB-linked substrates and l-DOPA. *Soil Biology and Biochemistry*, 41, 1180–1186. <https://doi.org/10.1016/j.soilbio.2009.02.029>

Dijkstra, F. A., Pendall, E., Morgan, J. A., Blumenthal, D. M., Carrillo, Y., LeCain, D. R., Follett, R. F., & Williams, D. G. (2012). Climate change alters stoichiometry of phosphorus and nitrogen in a semiarid grassland. *New Phytologist*, 196, 807–815. <https://doi.org/10.1111/j.1469-8137.2012.04349.x>

Dinerstein, E., Olson, D., Joshi, A., Vynne, C., Burgess, N. D., Wikramanayake, E., Hahn, N., Palminteri, S., Hedao, P., Noss, R., Hansen, M., Locke, H., Ellis, E. C., Jones, B., Barber, C. V., Hayes, R., Kormos, C., Martin, V., Crist, E., ... Saleem, M. (2017). An Ecoregion-based approach to protecting half the terrestrial realm. *BioScience*, 67, 534–545. <https://doi.org/10.1093/biosci/bix014>

Du, E., Terrer, C., Pellegrini, A. F. A., Ahlström, A., van Lissa, C. J., Zhao, X., Xia, N., Wu, X., & Jackson, R. B. (2020). Global patterns of terrestrial nitrogen and phosphorus limitation. *Nature Geoscience*, 13, 221–226. <https://doi.org/10.1038/s41561-019-0530-4>

ESRI. (2019). *ArcGIS desktop: Release 10.7.1*. Environmental Systems Research Institute.

Eyring, V., Bony, S., Meehl, G. A., Senior, C. A., Stevens, B., Stouffer, R. J., & Taylor, K. E. (2016). Overview of the Coupled Model Intercomparison Project Phase 6 (CMIP6) experimental design and organization. *Geoscientific Model Development*, 9, 1937–1958. <https://doi.org/10.5194/gmd-9-1937-2016>

Farrar, C. E., Tilman, D., Dybzinski, R., Reich, P. B., Levin, S. A., & Pacala, S. W. (2013). Resource limitation in a competitive context determines complex plant responses to experimental resource additions. *Ecology*, 94, 2505–2517. <https://doi.org/10.1890/12-1548.1>

Fick, S. E., & Hijmans, R. J. (2017). WorldClim 2: New 1-km spatial resolution climate surfaces for global land areas. *International Journal of Climatology*, 37, 4302–4315. <https://doi.org/10.1002/joc.5086>

German, D. P., Marcelo, K. R. B., Stone, M. M., & Allison, S. D. (2012). The Michaelis-Menten kinetics of soil extracellular enzymes in response to temperature: A cross-latitudinal study. *Global Change Biology*, 18, 1468–1479. <https://doi.org/10.1111/j.1365-2486.2011.02615.x>

German, D. P., Weintraub, M. N., Grandy, A. S., Lauber, C. L., Rinkes, Z. L., & Allison, S. D. (2011). Optimization of hydrolytic and oxidative enzyme methods for ecosystem studies. *Soil Biology and Biochemistry*, 43, 1387–1397. <https://doi.org/10.1016/j.soilbio.2011.03.017>

Gidden, M. J., Riahi, K., Smith, S. J., Fujimori, S., Luderer, G., Kriegler, E., van Vuuren, D. P., van den Berg, M., Feng, L., Klein, D., Calvin, K., Doelman, J. C., Frank, S., Fricko, O., Harmsen, M., Hasegawa, T., Havlik, P., Hilaire, J., Hoesly, R., ... Takahashi, K. (2019). Global emissions pathways under different socioeconomic scenarios for use in CMIP6: A dataset of harmonized emissions trajectories through the end of the century. *Geoscientific Model Development*, 12, 1443–1475. <https://doi.org/10.5194/gmd-12-1443-2019>

Galloway, J. N., Townsend, A. R., Erisman, J. W., Bekunda, M., Cai, Z., Freney, J. R., Martinelli, L. A., Setzinger, S. P., & Sutton, M. A. (2008). Transformations of the nitrogen cycle: Recent trends, questions, and potential solutions. *Science*, 320, 889–892. <https://doi.org/10.1126/science.1136674>

Hengl, T., Mendes de Jesus, J., Heuvelink, G. B., Ruiperez Gonzalez, M., Kilibarda, M., Blagotic, A., Shangguan, W., Wright, M. N., Geng, X., Bauer-Marschallinger, B., Guevara, M. A., Vargas, R., MacMillan, R. A., Batjes, N. H., Leenaars, J. G., Ribeiro, E., Wheeler, I., Mantel, S., & Kempen, B. (2017). SoilGrids250m: Global gridded soil information based on machine learning. *PLoS One*, 12, 1–40. <https://doi.org/10.1371/journal.pone.0169748>

Hicks Pries, C. E., Castanha, C., Porras, R. C., & Torn, M. S. (2017). The whole-soil carbon flux in response to warming. *Science*, 355, 1420–1423. <https://doi.org/10.1126/science.aal1319>

Hijmans, R. J. (2020). Raster: Geographic data analysis and modeling. R package version 3.4-5. <https://CRAN.R-project.org/package=raster>

Hothorn, T., Bretz, F., & Westfall, P. (2008). Simultaneous inference in general parametric models. *Biometrical Journal: Journal of Mathematical Methods in Biosciences*, 50, 346–363. <https://doi.org/10.1002/bimj.200810425>

Hou, E., Luo, Y., Kuang, Y., Chen, C., Lu, X., Jiang, L., Luo, X., & Wen, D. (2020). Global meta-analysis shows pervasive phosphorus limitation of aboveground plant production in natural terrestrial ecosystems. *Nature Communications*, 11, 1–9. <https://doi.org/10.1038/s41467-020-14492-w>

Hou, E., Wen, D., Jiang, L., Luo, X., Kuang, Y., Lu, X., Chen, C., Allen, K. T., He, X., Huang, X., & Luo, Y. (2021). Latitudinal patterns of terrestrial phosphorus limitation over the globe. *Ecology Letters*, 1–12. <https://doi.org/10.1111/ele.13761>

Hui, D., Mayes, M. A., & Wang, G. (2013). Kinetic parameters of phosphatase: A quantitative synthesis. *Soil Biology and Biochemistry*, 65, 105–113. <https://doi.org/10.1016/j.soilbio.2013.05.017>

Kelley, A. M., Fay, P. A., Polley, H. W., Gill, R. A., & Jackson, R. B. (2011). Atmospheric CO<sub>2</sub> and soil extracellular enzyme activity: A meta-analysis and CO<sub>2</sub> gradient experiment. *Ecosphere*, 2, 1–20. <https://doi.org/10.1890/ES11-00117.1>

Knorr, W., Prentice, I. C., House, J. I., & Holland, E. A. (2005). Long-term sensitivity of soil carbon turnover to warming. *Nature*, 433, 298–301. <https://doi.org/10.1038/nature03226>

Koch, O., Tscherko, D., & Kandeler, E. (2007). Temperature sensitivity of microbial respiration, nitrogen mineralization, and potential soil enzyme activities in organic alpine soils. *Global Biogeochemical Cycles*, 21, 1–11. <https://doi.org/10.1029/2007GB002983>

Koenker, R. (2021). Quantreg: Quantile regression. R package version 5.85. <https://CRAN.R-project.org/package=quantreg>

Lehmeier, C. A., Min, K., Niehues, N. D., Ballantyne, F., & Billings, S. A. (2013). Temperature-mediated changes of exoenzyme-substrate reaction rates and their consequences for the carbon to nitrogen flow ratio of liberated resources. *Soil Biology and Biochemistry*, 57, 374–382. <https://doi.org/10.1016/j.soilbio.2012.10.030>

Leprince, F., & Quiquampoix, H. (1996). Extracellular enzyme activity in soil: Effect of pH and ionic strength on the interaction with montmorillonite of two acid phosphatases secreted by the ectomycorrhizal fungus *Hebeloma cylindrosporum*. *European Journal of Soil Science*, 47, 511–522. <https://doi.org/10.1111/j.1365-2389.1996.tb01851.x>

Li, Y., Niu, S., & Yu, G. (2016). Aggravated phosphorus limitation on biomass production under increasing nitrogen loading: A meta-analysis. *Global Change Biology*, 22, 934–943. <https://doi.org/10.1111/gcb.13125>

Luo, Y., Ahlström, A., Allison, S. D., Batjes, N. H., Brovkin, V., Carvalhais, N., Chappell, A., Ciais, P., Davidson, E. A., Finzi, A., Georgiou, K., Guenet, B., Hararuk, O., Harden, J. W., He, Y., Hopkins, F., Jiang, L., Koven, C., Jackson, R. B., ... Zhou, T. (2016). Toward more realistic projections of soil carbon dynamics by Earth system models. *Global Biogeochemical Cycles*, 30, 40–56. <https://doi.org/10.1002/2015GBO05239>

Luo, Y., Hui, D., & Zhang, D. (2006). Elevated CO<sub>2</sub> stimulates net accumulations of carbon and nitrogen in land ecosystems: A meta-analysis. *Ecology*, 87, 53–63.

Mahowald, N., Jickells, T. D., Baker, A. R., Artaxo, P., Benitez-Nelson, C. R., Bergametti, G., Bond, T. C., Chen, Y., Cohen, D. D., Herut, B., Kubilay, N., Losno, R., Luo, C., Maenhaut, W., McGee, K. A., Okin, G. S., Siebert, R. L., & Tsukuda, S. (2008). Global distribution of atmospheric phosphorus sources, concentrations and deposition rates, and anthropogenic impacts. *Global Biogeochemical Cycles*, 22, 1–19. <https://doi.org/10.1029/2008GB003240>

Malik, A. A., Puissant, J., Buckeridge, K. M., Goodall, T., Jehmlich, N., Chowdhury, S., Gweon, H. S., Peyton, J. M., Mason, K. E., van Agtmaal, M., Blaud, A., Clark, I. M., Whitaker, J., Pywell, R. F., Ostle, N., Gleixner, G., & Griffiths, R. I. (2018). Land use driven change in soil pH affects microbial carbon cycling processes. *Nature Communications*, 9, 3591. <https://doi.org/10.1038/s41467-018-05980-1>

Manzoni, S., Moyano, F., Kätterer, T., & Schimel, J. (2016). Modeling coupled enzymatic and solute transport controls on decomposition in drying soils. *Soil Biology and Biochemistry*, 95, 275–287. <https://doi.org/10.1016/j.soilbio.2016.01.006>

Margalef, O., Sardans, J., Fernandez-Martinez, M., Molowny-Horas, R., Janssens, I. A., Ciais, P., Goll, D., Richter, A., Obersteiner, M., Asensio, D., & Penuelas, J. (2017). Global patterns of phosphatase activity in natural soils. *Scientific Reports*, 7, 1–13. <https://doi.org/10.1038/s41598-017-01418-8>

Marklein, A. R., & Houlton, B. Z. (2012). Nitrogen inputs accelerate phosphorus cycling rates across a wide variety of terrestrial ecosystems. *New Phytologist*, 193, 696–704. <https://doi.org/10.1111/j.1469-8137.2011.03967.x>

Mead, J. A. R., Smith, J. N., & Williams, R. T. (1955). Studies in detoxication. 67. The biosynthesis of the glucuronides of umbelliferone and 4-methylumbelliferone and their use in fluorimetric determination of  $\beta$ -glucuronidase. *Biochemical Journal*, 61, 569–574. <https://doi.org/10.1042/bj0610569>

Min, K., Buckeridge, K., Ziegler, S. E., Edwards, K. A., Bagchi, S., & Billings, S. A. (2019). Temperature sensitivity of biomass-specific microbial exo-enzyme activities and CO<sub>2</sub> efflux is resistant to change across short- and long-term timescales. *Global Change Biology*, 25, 1793–1807.

Min, K., Lehmeier, C. A., Ballantyne, F., Tatarko, A., & Billings, S. A. (2014). Differential effects of pH on temperature sensitivity of organic carbon and nitrogen decay. *Soil Biology and Biochemistry*, 76, 193–200. <https://doi.org/10.1016/j.soilbio.2014.05.021>

Olander, L. P., & Vitousek, P. M. (2000). Regulation of soil phosphatase and chitinase activity by N and P availability. *Biogeochemistry*, 49, 175–191. <https://doi.org/10.1023/A:1006316117817>

Penuelas, J., Poulter, B., Sardans, J., Ciais, P., van der Velde, M., Bopp, L., Boucher, O., Godderis, Y., Hinsinger, P., Llusia, J., Nardin, E., Vicca, S., Obersteiner, M., & Janssens, I. A. (2013). Human-induced nitrogen-phosphorus imbalances alter natural and managed ecosystems across the globe. *Nature Communications*, 4, 1–10. <https://doi.org/10.1038/ncomms3934>

Puissant, J., Jones, B., Goodall, T., Blaud, A., Gweon, H. S., Malik, A., Jones, D. L., Clark, I. M., Hirsch, P. R., & Griffiths, R. (2019). The pH optimum of soil exoenzymes adapt to long term changes in soil pH. *Soil Biology and Biochemistry*, 138, 1–9. <https://doi.org/10.1016/j.soilbio.2019.107601>

Quiquampoix, H. (2000). Mechanisms of protein adsorption on surfaces and consequences for extracellular enzyme activity in soil. In J. -M. Bollag & G. Stotzky (Eds.), *Soil biochemistry* (Vol. 10, pp. 171–206). Marcel Dekker.

R Core Team. (2020). *R: A language and environment for statistical computing*. R Foundation for Statistical Computing. <https://www.R-project.org/>

Rao, M. A., Violante, A., & Gianfreda, L. (2000). Interaction of acid phosphatase with clays, organic molecules and organo-mineral complexes: kinetics and stability. *Soil Biology and Biochemistry*, 32, 1007–1014. [https://doi.org/10.1016/S0038-0717\(00\)00010-9](https://doi.org/10.1016/S0038-0717(00)00010-9)

Razavi, B. S., Liu, S., & Kuzyakov, Y. (2017). Hot experience for cold-adapted microorganisms: Temperature sensitivity of soil enzymes. *Soil Biology and Biochemistry*, 105, 236–243. <https://doi.org/10.1016/j.soilbio.2016.11.026>

Reed, S. C., Yang, X., & Thornton, P. E. (2015). Incorporating phosphorus cycling into global modeling efforts: A worthwhile, tractable endeavor. *New Phytologist*, 208, 324–329. <https://doi.org/10.1111/nph.13521>

Sardans, J., Rivas-Ubach, A., & Peñuelas, J. (2012). The C:N:P stoichiometry of organisms and ecosystems in a changing world: A review and perspectives. *Perspectives in Plant Ecology, Evolution and Systematics*, 14, 33–47. <https://doi.org/10.1016/j.ppees.2011.08.002>

Schimel, J., Balser, T. C., & Wallenstein, M. (2007). Microbial stress-response physiology and its implications for ecosystem function. *Ecology*, 88, 1386–1394. <https://doi.org/10.1890/06-0219>

Sinsabaugh, R. L. (2010). Phenol oxidase, peroxidase and organic matter dynamics of soil. *Soil Biology and Biochemistry*, 42, 391–404. <https://doi.org/10.1016/j.soilbio.2009.10.014>

Sinsabaugh, R. L., Lauber, C. L., Weintraub, M. N., Ahmed, B., Allison, S. D., Crenshaw, C., Contosta, A. R., Cusack, D., Frey, S., Gallo, M. E., Gartner, T. B., Hobbie, S. E., Holland, K., Keeler, B. L., Powers, J. S., Stursova, M., Takacs-Vesbach, C., Waldrop, M. P., Wallenstein, M. D., ... Zeglin, L. H. (2008). Stoichiometry of soil enzyme activity at global scale. *Ecology Letters*, 11, 1252–1264. <https://doi.org/10.1111/j.1461-0248.2008.01245.x>

Slessarev, E. W., Lin, Y., Bingham, N. L., Johnson, J. E., Dai, Y., Schimel, J. P., & Chadwick, O. A. (2016). Water balance creates a threshold in soil pH at the global scale. *Nature*, 540, 567–569. <https://doi.org/10.1038/nature20139>

Sokolov, A. P., Kicklighter, D. W., Melillo, J. M., Felzer, B. S., Schlosser, C. A., & Cronin, T. W. (2008). Consequences of considering carbon-nitrogen interactions on the feedbacks between climate and the terrestrial carbon cycle. *Journal of Climate*, 21, 3776–3796. <https://doi.org/10.1175/2008JCLI2038.1>

Steinweg, J. M., Dukes, J. S., Paul, E. A., & Wallenstein, M. D. (2013). Microbial responses to multi-factor climate change: Effects on soil enzymes. *Frontiers in Microbiology*, 4, 1–11. <https://doi.org/10.3389/fmicb.2013.00146>

Steinweg, J. M., Jagadamma, S., Frerichs, J., & Mayes, M. A. (2013). Activation energy of extracellular enzymes in soils from different biomes. *PLoS One*, 8, 1–7. <https://doi.org/10.1371/journal.pone.0059943>

Sun, Y., Peng, S., Goll, D. S., Ciais, P., Guenet, B., Guimbertea, M., Hinsinger, P., Janssens, I. A., Peñuelas, J., Piao, S., Poulter, B., Violette, A., Yang, X., Yin, Y., & Zeng, H. (2017). Diagnosing phosphorus limitations in natural terrestrial ecosystems in carbon cycle models. *Earth's Future*, 5, 730–749. <https://doi.org/10.1002/2016EF000472>

Thornton, P. E., Lamarque, J.-F., Rosenbloom, N. A., & Mahowald, N. M. (2007). Influence of carbon-nitrogen cycle coupling on land model response to CO<sub>2</sub> fertilization and climate variability. *Global Biogeochemical Cycles*, 21, 1–15. <https://doi.org/10.1029/2006GB002868>

Tiemann, L. K., & Billings, S. A. (2011). Changes in variability of soil moisture alter microbial community C and N resource use. *Soil Biology and Biochemistry*, 43, 1837–1847. <https://doi.org/10.1016/j.soilbio.2011.04.020>

Treseder, K. K., Allen, E. B., Egerton-Warburton, L. M., Hart, M. M., Klironomos, J. N., Maherli, H., Tedersoo, L., & Wurzburger, N. (2018). Arbuscular mycorrhizal fungi as mediators of ecosystem responses to nitrogen deposition: A trait-based predictive framework. *Journal of Ecology*, 106, 480–489. <https://doi.org/10.1111/1365-2745.12919>

Vitousek, P. M., Porder, S., Houlton, B. Z., & Chadwick, O. A. (2010). Terrestrial phosphorus limitation: Mechanisms, implications, and nitrogen-phosphorus interactions. *Ecological Applications*, 20, 5–15. <https://doi.org/10.1890/08-0127.1>

von Lützow, M., & Kögel-Knabner, I. (2009). Temperature sensitivity of soil organic matter decomposition—What do we know? *Biology and Fertility of Soils*, 46, 1–15. <https://doi.org/10.1007/s00374-009-0413-8>

Walker, T. W., & Syers, J. K. (1976). The fate of phosphorus during pedogenesis. *Geoderma*, 15(1), 1–19. [https://doi.org/10.1016/0016-7061\(76\)90066-5](https://doi.org/10.1016/0016-7061(76)90066-5)

Wallenstein, M. D., Allison, S. D., Ernakovich, J., Steinweg, J. M., & Sinsabaugh, R. (2010). Controls on the temperature sensitivity of soil enzymes: A key driver of in situ enzyme activity rates. In G. Shukla & A. Varma (Eds.), *Soil enzymology*. *Soil biology* (Vol. 22, pp. 245–258). Springer. [https://doi.org/10.1007/978-3-642-14225-3\\_13](https://doi.org/10.1007/978-3-642-14225-3_13)

Wallenstein, M. D., & Weitbraub, M. N. (2008). Emerging tools for measuring and modeling the in situ activity of soil extracellular enzymes. *Soil Biology and Biochemistry*, 9, 2098–2106. <https://doi.org/10.1016/j.soilbio.2008.01.024>

Wang, Y. P., Law, R. M., & Pak, B. (2010). A global model of carbon, nitrogen and phosphorus cycles for the terrestrial biosphere. *Biogeosciences*, 7, 2261–2282. <https://doi.org/10.5194/bg-7-2261-2010>

Wieder, W. R., Allison, S. D., Davidson, E. A., Georgiou, K., Hararuk, O., He, Y., Hopkins, F., Luo, Y., Smith, M. J., Sulman, B., Todd-Brown, K., Wang, Y.-P., Xia, J., & Xu, X. (2015). Explicitly representing soil microbial processes in Earth system models. *Global Biogeochemical Cycles*, 29, 1782–1800. <https://doi.org/10.1002/2015GB005188>

Wieder, W. R., Hartman, M. D., Sulman, B. N., Wang, Y. P., Koven, C. D., & Bonan, G. B. (2018). Carbon cycle confidence and uncertainty: Exploring variation among soil biogeochemical models. *Global Change Biology*, 24, 1563–1579. <https://doi.org/10.1111/gcb.13979>

Xiao, W., Chen, X., Jing, X., & Zhu, B. (2018). A meta-analysis of soil extracellular enzyme activities in response to global change. *Soil Biology and Biochemistry*, 123, 21–32. <https://doi.org/10.1016/j.soilbio.2018.05.001>

Yue, K., Fornara, D. A., Yang, W., Peng, Y., Li, Z., Wu, F., & Peng, C. (2017). Effects of three global change drivers on terrestrial C:N:P stoichiometry: A global synthesis. *Global Change Biology*, 23, 2450–2463. <https://doi.org/10.1111/gcb.13569>

Zaehele, S., Friend, A. D., Friedlingstein, P., Dentener, F., Peylin, P., & Schulz, M. (2010). Carbon and nitrogen cycle dynamics in the O-CN land surface model: 2. Role of the nitrogen cycle in the historical terrestrial carbon balance. *Global Biogeochemical Cycles*, 24, 1–14. <https://doi.org/10.1029/2009GB003522>

Zimmerman, A. R., & Ahn, M. (2010). Organo-mineral-enzyme interaction and soil enzyme activity. In G. Shukla & A. Varma (Eds.), *Soil enzymology*. *Soil biology* (Vol. 22, pp. 271–292). Springer. [https://doi.org/10.1007/978-3-642-14225-3\\_15](https://doi.org/10.1007/978-3-642-14225-3_15)

## SUPPORTING INFORMATION

Additional supporting information may be found in the online version of the article at the publisher's website.

**How to cite this article:** de Souza, L. F. T., & Billings, S. A. (2021). Temperature and pH mediate stoichiometric constraints of organically derived soil nutrients. *Global Change Biology*, 00, 1–13. <https://doi.org/10.1111/gcb.15985>